Hypothetical control of postural sway

Madhur Mangalam[a,*] and Damian G. Kelty-Stephen[b,†]

[a]Department of Physical Therapy, Movement and Rehabilitation Sciences, Northeastern University, Boston, MA 02115, USA

[b]Department of Psychology, Grinnell College, Grinnell, IA 50112, USA

[*]Corresponding author at: Department of Physical Therapy, Movement and Rehabilitation Sciences, Northeastern University, Boston, MA 02115, USA.

E-mail addresses: m.mangalam@northeastern.edu (M. Mangalam).

[†]Corresponding author at: Department of Psychology, Grinnell College, Grinnell, IA 50112, USA.

E-mail addresses: keltysda@grinnell.edu (D. G. Kelty-Stephen).

Abstract

Quiet standing exhibits strongly intermittent variability reflecting a richly interactive foundation. This intermittency can be understood in various ways. First, variability can be intermittent through the engagement and disengagement of complementary control processes at distinct scales. A second and perhaps a deeper way to understand this intermittency is through the possibility that closed-loop control depends on the cascade-like interactions across many timescales at once. These diverse control processes suggest specific non-Gaussian distributional properties at different timescales. Multiscale probability density (PDF) analysis shows that quiet standing on a stable surface exhibits a crossover between low non-Gaussianity (consistent with exponential distributions) at shorter timescales reflecting open-loop control, increasing towards higher non-Gaussianity and subsequently decreasing (consistent with cascade-driven Lévy-like distributions) at longer scales. Destabilizing quiet standing elicits non-Gaussianity that begins high and decreases across timescales (consistent with cascade-driven Lévy-like distribution), reflecting closed-loop postural corrections at more of the shorter timescales. Finally, indices of postural sway govern the appearance or disappearance of crossovers, suggesting that tempering of non-Gaussianity across log-timescale in stable-surface condition is mostly a function of endogenous postural control. These results provide new evidence that cascading interactions across longer-timescales supporting postural corrections can even recruit shorter-timescale processes with novel task constraints.

Keywords: center of pressure; inverse power law; postural control; scale invariance; quite stance; Lévy walk

1. Introduction

1.1. Postural sway in quiet standing

Quiet standing—a fundamental motor act that provides the basis for other movement tasks—exhibits strongly intermittent variability reflecting a richly interactive foundation. This intermittency can be understood in various ways. First, variability can be intermittent through the engagement and disengagement of complementary control processes. For instance, during quiet standing, the body continually sways about a constant average position of the global ground reaction force (center of pressure, CoP) trajectory. Within the center of the base of upright support, bodily sway respects the so-called open-loop control, but at longer scales, towards the margins of the base of support, the postural system relies on the so-called closed-loop control to generate postural corrections based on sensory feedback [1,2]. A second and perhaps a deeper way to understand this intermittency is through the possibility that closed-loop control depends on the cascade-like interactions across many timescales. For instance, quiet standing involves the integration of information from visual, vestibular, and somatosensory receptors, in conjunction with the passive properties of the musculoskeletal system. The neurological and physiological processes that have been suggested to dictate intermittency in postural sway include active mechanical processes [3–5], passive reflex mechanisms [6,7] anticipatory [8–10] and feedback processes [11,12], and exploratory processes used by the central nervous system (CNS) to generate sensory information [13,14].

The sources of intermittency noted above should each entail characteristic signatures on the distributional properties of postural sway. Specifically, shorter-timescale sway that roams 'unchecked' within a limited range resembles Brownian motion [1,2], indicated by strong temporal correlations across steps whose nonzero size is drawn from the thin-tailed, finite-variance (e.g., exponential) distributions [15]. The use of feedback to correct motor performance as in longer-timescale sway reflects weaker correlations across steps drawn from non-Gaussian distributions reflecting multiplicative random processes [16]. These distributions are 'Lévy-like,' showing heavy scale-invariant tails potentially tempered with finite variance (e.g., lognormal) or potentially having infinite variance (untempered Lévy-stable) [17]. That is, quiet standing should exhibit exponential distributions at smaller timescales and Lévy-like distributions at longer timescales devoted to postural corrections.

The present work probes postural sway in quiet standing for precisely this crossover from shorter-scale exponential distribution to larger-scale non-Gaussianity. Given the known tradeoffs between temporal correlations and Lévy-like scaling [18,19], this hypothetical crossover in non-Gaussianity could serve as a complement to the crossover in temporal correlations [20,21]. To ensure that the crossover is specific to the timescale-dependence of postural corrections, we examine multiscale non-Gaussianity under manipulations intended to destabilize posture and thus to elicit postural corrections into the short scales traditionally associated with so-called open-loop control.

1.2. Multiscale probability density function (PDF) analysis of postural sway in quiet standing

A central feature of intermittent, cascading fluctuations is the heterogeneity of variance, across space and time scales, beyond the bounds of a Gaussian distribution. Research on intermittency in the turbulent fluid flow inspired a method for quantifying this heterogeneity of variance through a metric λ_s^2 [22]. For timescale-invariant cascading form, λ_s^2 begins at higher values for short timescales and decreases monotonically with the natural logarithm of

timescale. This method has successfully quantified differences in non-Gaussianity in heart-rate variability (HRV) with pathology [23–27] and in neuronal interspike intervals (ISI) with sleep/wake cycles [28].

Beyond aligning physiological cascades with hydrodynamic cascades, non-Gaussianity affords close empirical relationships with more traditional physiological measures. Results for both HRV and ISI suggested that endogenous control processes might account for the variability in λ_s^2 vs. log-timescale curves. For instance, endogenous sinoatrial dynamics could explain the tempering of Lévy PDFs in healthy controls compared to Lévy-stable PDFs for pathological cases in HRV [29], and non-Gaussianity showed relationships with the magnitude autocorrelation of the ISI [28]. Hence, besides testing whether corrections in different scales in quiet standing changes non-Gaussianity of CoP dynamics, we can test whether manipulations of and endogenous variability in postural control could produce a quantifiable change in cascade-structure.

We apply multiscale PDF method to study postural control and test three specific hypotheses in a reanalysis of a public dataset of kinematics and ground reaction forces [30]. Hypothesis 1 is that quiet standing on a stable surface would show a crossover between low non-Gaussianity (consistent with exponential distributions) at shorter timescales reflecting open-loop control, increasing towards higher and subsequently decreasing (consistent with cascade-driven Lévy-like distributions) at longer scales. Specifically, we tested for this crossover as a negative quadratic polynomial with log-timescale. Hypothesis 2 is that destabilizing quiet standing should require closed-loop postural corrections at more of the shorter timescales, eliciting non-Gaussianity that begins high and decreases across timescales (consistent with cascade-driven Lévy-like distribution). Specifically, we expected that quite standing on an unstable surface or closing eyes would cancel this negative quadratic polynomial. Hypothesis 3 is that indices of postural control would significantly moderate the quadratic polynomial, effectively governing the appearance or disappearance of the crossover.

2. Methods

2.1. Participants

Forty nine participants grouped by age: young (15 males and 12 females, 18–40 years old) and old (11 males and 11 females, > 60 years old) took part in the study after providing informed consent.

2.2. Experimental setup and procedure

Each participant stood still for 60 s under all four possible combinations of vision (eyes open/eyes closed) and standing surface (stable/unstable). Stable condition involved standing on two 40×60 cm force platforms (100 Hz, OPT400600-1000; AMTI Inc., Watertown, MA) under each foot, and in unstable condition, the participants stood on two 6-cm high foam blocks (Balance Pad, Airex AG Inc., Sins, Switzerland), each placed on each force platform.

2.3. Data processing

All data processing was performed in MATLAB 2019b (Matlab Inc., Natick, MA). Trial-by-trial ground reaction forces yielded a 2D center of pressure (CoP) series, each dimension describing CoP position along anterior-posterior (AP) and medial-lateral (ML) axes. Each 60-s trial yielded 6000-sample 2D CoP series and 5999-sample 2D CoP displacement series. Finally, a 1D CoP planar Euclidean displacement (PED) series described postural sway along

the transverse plane of the body. Iterated Amplitude Adjusted Fourier Transformation (IAAFT) provided phase-randomized surrogates a surrogate series using original series' spectral amplitudes to preserve only linear temporal correlations [31,32].

2.4. Canonical indices of postural sway

Three linear indices were computed for each CoP PED series: (i) Mean of all fluctuations (CoP_PED_*Mean*), (ii) Standard deviation (CoP_PED_*SD*), and (iii) Root mean square (CoP_PED_*RMSE*).

Four nonlinear indices were computed for each CoP PED series: (i) Sample entropy (CoP_PED_*SampEn*), indexing the extent of complexity in the signal [33]. We used m = 2 and r = 0.2 for computing the *SampEn* [cf. 34]. (ii) Multiscale sample entropy (CoP_PED_*MSE*), indexing signal complexity over multiple timescales [35]. We used m = 2, r = 0.2, and τ = 20 for computing the *MSE* [cf. 34]. (iii) We used detrended fluctuation analysis [36] to compute Hurst's exponent, H_{fGn}, indexing temporal correlations in original CoP PED series (CoP_PED_$H_{\mathrm{fGn_Original}}$) and shuffled versions of each series (CoP_PED_$H_{\mathrm{fGn_Shuffled}}$) using the scaling region: 4, 8, 12,… 1024 [cf. 37]. Shuffling destroys the temporal structure of a signal. (iv) Multifractal spectrum width, $\Delta\alpha$, indexing the extent of multifractal temporal correlations in the signal. Chhabra and Jensen's direct method [38] was used to compute $\Delta\alpha$ for the original CoP series (CoP_PED_$\Delta\alpha_{\mathrm{Original}}$) and the IAAFT surrogate (CoP_PED_$\Delta\alpha_{\mathrm{Surrogate}}$) [cf. 38].

2.5. Multiscale probability density function (PDF) analysis

Multiscale PDF analysis characterizes the distribution of abrupt changes in CoP PED series { $b(t)$ } using the PDF tail. The first step is to generate { $B(t)$ } by integrating { $b(t)$ } after centering by the mean b_{ave} (Fig. 1, top):

$$B(t)=\sum_{i=1}^{t/\Delta t} b(i\Delta t)-b_{ave} \quad .$$

A a 3rd order polynomial detrends { $B(t)$ } within k overlapping windows of length $2s$, s being the timescale (Fig. 1, middle). Intermittent deviation $\Delta_s B(t)$ in k^{th} window from $1+s(k-1)$ to sk in the detrended time series { $B^d(t)=B(t)-f_{fit}(t)$ } is computed as $\Delta_s B^d(t)=B^d(t+s)-B^d(t)$, where $1+s(k-1)\leq t\leq sk$ and $f_{fit}(t)$ is the polynomial representing the local trend of { $B(t)$ }, of which the elimination assures the zero-mean probability density function in the next step (Fig. 1, bottom). Finally, $\Delta_s B$ is normalized by the SD (i.e., variance is set to one) to quantify the PDF.

To quantify the non-Gaussianity of $\Delta_s B$ at timescale s, the standardized PDF constructed from all the $\Delta_s B(t)$ values is approximated by the Castaing model,[22] with λ_s as a single parameter characterizing the non-Gaussianity of the PDF. λ_s is estimated as

$$\lambda_s^2=\frac{2}{q(q-2)}\left[\ln\left(\sqrt{\pi}\langle|\Delta_s B|^q\rangle\right)+\ln\Gamma\left(\frac{q+1}{2}\right)-\frac{q}{2}\ln 2\right] \quad ,$$

where $\langle|\Delta_s B|^q\rangle$ denotes an estimated value of qth order absolute moment of { $\Delta_s B$ }. As λ_s increases, the PDF becomes increasingly peaked and fat-tailed (Fig. 2, left). λ_s can be estimated by Eq. (7) based on q^{th} order absolute moment of a time series independent of q. Estimating λ_s based on 0.2th moment (q = 0.2) emphasizes the center part of the PDF, reducing the effects of extreme deviations due to heavy-tails and kurtosis. We used

0.2th moment because estimates of λ_s for a time series of 6000 are more accurate at lower values of q [40].

Cascade-type multiplicative process yield the inverse relationship $\lambda_s^2 \sim -\ln s$ [25]. For the present purposes, we quantified λ_s for each original CoP SED series and corresponding IAAFT surrogate at timescales 5 to 1000 samples (i.e., 50 ms to 10 s) at steps of 5 samples (50 ms). We used Akaike Information Criterion (AIC) weights to determine whether the PDF at each timescale was a power law, lognormal, exponential, or gamma distribution.

2.6. Statistical analysis

To test for crossovers in non-Gaussianity, a linear mixed-effect (LME) model using lmer [41] in R package "lme4" tested λ_s^2 vs. log-timescale curves for orthogonal linear and quadratic polynomials, for interactions with grouping variables (Age×Surface×Vision×Original, where Original encoded differences in original series from surrogates) and with indices of postural sway (Section 2.4.). Statistical significance was assumed at the alpha level of 0.05 using R package "lmerTest" [42]. To test how lognormality changed with log-timescale, a generalized linear mixed-effect (GLME) fit changes in Lognormality as a dichotomous variable using orthogonal linear, quadratic, and cubic polynomials and tested interaction effects of grouping variables (Age×Surface×Vision×Original) with those polynomials using glmer [43] in lme4.

3. Results

Figs. 3 and 4 provide a schematic of multiscale PDF characterization of postural sway in representative young and old participants standing quietly for 60 s on stable and unstable surfaces with eyes closed (Fig. 3) and eyes open (Fig. 4). Fig. 5 exemplifies PDFs at timescales ranging from 50 ms to 10 s, obtained from multiscale PDF analysis for a representative original CoP PED series and its IAAFT surrogate. Note the difference in PDF with increasing timescale between original and surrogate series.

3.1. Effects of Age×Surface×Vision on λ_s^2 vs. log-timescale curves

Surface stability elicited nonlinearity in non-Gaussianity with timescale, that is, low short-scale non-Gaussianity, increasing up to a maximum roughly at 75 samples (750 ms), and decreasing with subsequently longer timescales (Table S1; Fig. 6, left). Non-Gaussianity showed stronger linear decrease (B = –13.37, P < 0.001) and downward-facing parabolic shape (B = –2.57, P < 0.001) for the old participants in stable-surface/eyes-open condition. The young participants showed a significantly shallower linear decrease in stable-surface non-Gaussianity with longer timescale (B = 3.75, P < 0.001). Changes in the nonlinearity of non-Gaussianity with log-timescale did not depend on age or differ between eyes-open and eyes-closed conditions (P > 0.05). Additionally, the young participants showed a marginally significant tendency to show a more negative, more downward-opening parabolic shape in stable-surface/eyes-closed condition (B = –1.36, P = 0.054).

Surface instability elicited characteristic evidence of robust scale invariance, that is, higher non-Gaussianity at shorter timescales with persistent decreases with increasing timescales (Fig. 6, right). The most robust scale-invariant behavior appeared in the unstable-surface/eyes-closed condition irrespective of the participants' age. Non-Gaussianity showed stronger linear decreases for the older participants with eyes open (B = –5.37, P < 0.001)

and, to a lesser extent, for the young participants with eyes open (B = –3.26, P = 0.001). In unstable-surface conditions, non-Gaussianity showed no downward-facing parabolic shape as in stable-surface conditions. The old participants showed stronger downward-facing parabolic shape with eyes open (B = 8.64, P < 0.001) and eyes closed (B = 3.26, P < 0.001) conditions. The young participants showed significantly shallower parabolic decay in non-Gaussianity (B = –1.67, P = 0.018) with a relatively weak positive effect with eyes open (B = 0.0069, P < 0.001).

All indices of postural sway showed predictive effects on non-Gaussianity (Table S1). Non-Gaussianity typically decreased with increases in CoP_PED_*Mean*, CoP_PED_*SD*, CoP_PED_*SampEn*, and CoP_PED_*MSE*, and increased with increases in CoP_PED_*RMSE* (Table S2). It also increased with both the strength of temporal correlations or fractality (i.e., CoP_PED_$H_{\mathrm{fGn_Original}}$) and more variation in these temporal correlations or multifractality (i.e., CoP_PED_$\Delta\alpha_{\mathrm{Original}}$). Nonetheless, in the tradeoff between temporal correlations and Lévy-like statistics, greater 'original-minus-surrogate' differences in both fractality and multifractality diminished non-Gaussianity. This result confirms the fact that evidence of multifractality with a relatively weak difference from the surrogates suggests heavy-tailed distributions and thus non-Gaussianity [26,27]. However, this model, including only the main effects of these indices, speaks only to average differences in λ_2^2 and not to the trajectory of λ_2^2 across log-timescale.

Including the interactions of all indices of postural sway with linear and quadratic terms in the prior model significantly improved the model fit (χ^2_{423} = 32699, P < 0.001; Table S2). Table S2 details the full model, but in short, it illustrated two major points: first, most of the variability in the quadratic form of the λ_2^2 vs. log-timescale curves depended on these indices. This newer model with interactions of these indices with log-timescale had 69 significant quadratic effects (P < 0.05) and ten quadratic effects approaching significance (0.05 ≤ P < 0.10), and all but one significant and two approaching-significant quadratic effects were interactions of these indices with log-timescale. That is, the parabolic tempering of non-Gaussianity across log-timescale in stable-surface condition was mostly a function of endogenous postural control.

3.2. Effects of Age×Surface×Vision on growth of lognormality in postural sway with log-timescale

The original CoP PED series exhibited less lognormality overall than the surrogates (B = –1.74, P < 0.001; Table S3; Fig. 7).

First, surface stability yielded faster growth in lognormality for the old than the young participants (Fig. 7, left). For the old participants in stable-surface/eyes-open condition, the CoP PED series showed a stronger positive linear (B = 296.17, P < 0.001) and quadratic (B = 161.98, P < 0.001), but a negative cubic (B = –209.17, P = < 0.001) growth with log-timescale. This polynomial profile for stable surface did not vary for the young participants or all participants with eyes closed, except for showing less lognormality overall (B = –0.42, P < 0.0001; B = –0.41, P < 0.0001, respectively).

Second, surface instability made the growth of lognormality with log-timescale more similar between the young and old participants (Fig. 7, right), showing greater lognormality in the young participants (B = 0.37, P = 0.002) and for all participants with eyes closed (B = 0.62, P < 0.001). Also, surface instability made the quadratic growth with log-timescale weaker with eyes open (B = –248.63, P = 0.042) and stronger with eyes closed (B = 417.71, P = 0.041). Effects of surface instability depended on age, with closed eyes accentuating the

cubic relationship with log-timescale for the old participants (B = –231.45, P = 0.027) but reversing it for the young participants (B = 353.97, P = 0.040).

4. Discussion

Multiscale PDF analysis tested whether postural sway exhibits correlated-random and Lévy walks at relatively short and relatively long scales. Our major finding is that of a crossover in non-Gaussianity profiles of postural sway with timescale. This crossover likely reflects a transition between correlated and uncorrelated random walks reflecting distinct control processes. This analogy makes the most sense in the light of the fact that the non-Gaussianity index λ_2^2 is conceptually inverse to the Hurst exponent H_{fGn} relating variance to timescale. As noted above, the power-law structure in the Lévy-like PDF often appears at the expense of power-law temporal correlations [18]. The present work joins a growing enterprise in attempting to characterize diverse control processes through nonlinear methods. Importantly, for attempts to characterize this diversity of control, the capacity of non-Gaussianity to spread from the longer scales into shorter scales with unstable surfaces offers new grounds for doubting whether an open-/closed-loop distinction is fundamental [1,2,20,21]. Sensory processes and postural corrections do not necessarily observe a firm divide between fast and slow processes. Instead, postural control reflects a richly interactive capacity for movement organization to emerge through the coordination of multiple scales [44,45].

It has been shown that healthy human postural sway exhibits fractality [46] and multifractality [47]. Using multiscale PDF analysis in the present study, we show that healthy human postural sway is more compatible with the cascade-type multiplicative model. Crucially, we add that at specific timescales, it shows signatures of two competing processes. On the one hand, the reduction in non-Gaussianity with timescale indicates a cascade-type multiplicative process with less deviation in the magnitude of fluctuations. On the other hand, the change in PDF from exponential to lognormal at sufficiently longer timescales indicates a higher potential of heavy-tailed fluctuations at these longer timescales. Based on this crossover, we hypothesize that intermittency in postural sway at longer timescales can potentially lead to falls in individuals with deficits in the postural control system. Future work could test this hypothesis using multiscale PDF analysis in clinical populations.

In conclusion, we show that quiet standing on a stable surface shows a crossover between low non-Gaussianity (consistent with exponential distributions) at shorter timescales reflecting open-loop control, increasing towards higher and subsequently decreasing (consistent with cascade-driven Lévy-like distributions) at longer scales. Destabilizing quiet standing elicits non-Gaussianity that begins high and decreases across timescales (consistent with cascade-driven Lévy-like distribution), reflecting closed-loop postural corrections at more of the shorter timescales. Finally, indices of postural control govern the appearance or disappearance of the crossover. Likewise, multiscale PDF analysis could be a useful analytical technique to identify the timescales over which the temporal correlations in a physiological activity switch to Lévy-like processes with no finite variance. The heavy-tailed fluctuations implied by this switch have life-and-death consequences for healthy functioning (e.g., preventing falls, reducing cardiac pathology, etc.). These fluctuations should be a topic of future work.

Supplementary material

Table S1. Coefficients of linear mixed-effect (LME) model examining effects of Age×Surface×Vision on λ_s^2 vs. log-timescale curves.

Table S2. Coefficients of LME model examining effects of Age×Surface×Vision on λ_s^2 vs. log-timescale curves for orthogonal linear and quadratic polynomials, for interactions of grouping variables (Age×Surface×Vision×Original) and with indices of postural sway.

Table S3. Coefficients of generalized linear mixed-effect (GLME) model examining effects of Age×Surface×Vision×Original on growth of lognormality in postural sway with log-timescale.

Author contributions

M.M. and D.G.K-S. conceived and designed research; M.M. and D.G.K-S. analyzed data; M.M. and D.G.K-S. interpreted results of experiments; M.M. prepared figures; M.M. and D.G.K-S. drafted manuscript; M.M. and D.G.K-S. edited and revised manuscript; M.M. and D.G.K-S. approved final version of manuscript.

References

[1] J.J. Collins, C.J. De Luca, Open-loop and closed-loop control of posture: A random-walk analysis of center-of-pressure trajectories, Exp. Brain Res. 95 (1993) 308–318. https://doi.org/10.1007/BF00229788.

[2] J.J. Collins, C.J. De Luca, Upright, correlated random walks: A statistical-biomechanics approach to the human postural control system, Chaos An Interdiscip. J. Nonlinear Sci. 5 (1995) 57–63. https://doi.org/10.1063/1.166086.

[3] D.A. Winter, Human balance and posture control during standing and walking, Gait Posture. 3 (1995) 193–214. https://doi.org/10.1016/0966-6362(96)82849-9.

[4] D.A. Winter, A.E. Patla, M. Ishac, W.H. Gage, Motor mechanisms of balance during quiet standing, J. Electromyogr. Kinesiol. 13 (2003) 49–56. https://doi.org/10.1016/S1050-6411(02)00085-8.

[5] D.A. Winter, A.E. Patla, F. Prince, M. Ishac, K. Gielo-Perczak, Stiffness control of balance in quiet standing, J. Neurophysiol. 80 (1998) 1211–1221. https://doi.org/10.1152/jn.1998.80.3.1211.

[6] R. Fitzpatrick, D. Burke, S.C. Gandevia, Loop gain of reflexes controlling human standing measured with the use of postural and vestibular disturbances, J. Neurophysiol. 76 (1996) 3994–4008. https://doi.org/10.1152/jn.1996.76.6.3994.

[7] A.M. Bacsi, J.G. Colebatch, Evidence for reflex and perceptual vestibular contributions to postural control, Exp. Brain Res. 160 (2005) 22–28. https://doi.org/10.1007/s00221-004-1982-2.

[8] G.N. Gantchev, D.M. Dimitrova, Anticipatory postural adjustments associated with arm movements during balancing on unstable support surface, Int. J. Psychophysiol. 22 (1996) 117–122. https://doi.org/10.1016/0167-8760(96)00016-5.

[9] M. Klous, P. Mikulic, M.L. Latash, Two aspects of feedforward postural control: Anticipatory postural adjustments and anticipatory synergy adjustments, J. Neurophysiol. 105 (2011) 2275–2288. https://doi.org/10.1152/jn.00665.2010.

[10] M. Klous, P. Mikulic, M.L. Latash, Early postural adjustments in preparation to whole-body voluntary sway, J. Electromyogr. Kinesiol. 22 (2012) 110–116. https://doi.org/10.1016/j.jelekin.2011.11.005.

[11] R.J. Peterka, P.J. Loughlin, Dynamic regulation of sensorimotor integration in human postural control, J. Neurophysiol. 91 (2004) 410–423. https://doi.org/10.1152/jn.00516.2003.

[12] R.J. Peterka, Sensorimotor integration in human postural control, J. Neurophysiol. 88 (2002) 1097–1118. https://doi.org/10.1152/jn.2002.88.3.1097.

[13] M.G. Carpenter, C.D. Murnaghan, J.T. Inglis, Shifting the balance: Evidence of an exploratory role for postural sway, Neuroscience. 171 (2010) 196–204. https://doi.org/10.1016/j.neuroscience.2010.08.030.

[14] C.D. Murnaghan, B.C. Horslen, J.T. Inglis, M.G. Carpenter, Exploratory behavior during stance persists with visual feedback, Neuroscience. 195 (2011) 54–59. https://doi.org/10.1016/j.neuroscience.2011.08.020.

[15] E.A. Codling, M.J. Plank, S. Benhamou, Random walk models in biology, J. R. Soc. Interface. 5 (2008) 813–834. https://doi.org/10.1098/rsif.2008.0014.

[16] N. Kuznetsov, S. Wallot, Effects of accuracy feedback on fractal characteristics of time estimation, Front. Integr. Neurosci. 5 (2011) 62. https://doi.org/10.3389/fnint.2011.00062.

[17] D.W. Sims, E.J. Southall, N.E. Humphries, G.C. Hays, C.J.A. Bradshaw, J.W. Pitchford, A. James, M.Z. Ahmed, A.S. Brierley, M.A. Hindell, D. Morritt, M.K. Musyl, D. Righton, E.L.C. Shepard, V.J. Wearmouth, R.P. Wilson, M.J. Witt, J.D. Metcalfe, Scaling laws of marine predator search behaviour, Nature. 451 (2008) 1098–1102. https://doi.org/10.1038/nature06518.

[18] N. Scafetta, P. Grigolini, Scaling detection in time series: Diffusion entropy analysis, Phys. Rev. E. 66 (2002) 36130. https://doi.org/10.1103/PhysRevE.66.036130.

[19] A.M. Reynolds, Truncated Lévy walks are expected beyond the scale of data collection when correlated random walks embody observed movement patterns, J. R. Soc. Interface. 9 (2012) 528–534. https://doi.org/10.1098/rsif.2011.0363.

[20] P. Federolf, P. Zandiyeh, V. von Tscharner, Time scale dependence of the center of pressure entropy: What characteristics of the neuromuscular postural control system influence stabilographic entropic half-life?, Exp. Brain Res. 233 (2015) 3507–3515. https://doi.org/10.1007/s00221-015-4420-8.

[21] D. Delignières, K. Torre, P.-L. Bernard, Transition from persistent to anti-persistent correlations in postural sway indicates velocity-based control, PLOS Comput. Biol. 7 (2011) e1001089. https://doi.org/10.1371/journal.pcbi.1001089.

[22] B. Castaing, Y. Gagne, E.J. Hopfinger, Velocity probability density functions of high Reynolds number turbulence, Phys. D Nonlinear Phenom. 46 (1990) 177–200. https://doi.org/10.1016/0167-2789(90)90035-N.

[23] K. Kiyono, Z.R. Struzik, N. Aoyagi, S. Sakata, J. Hayano, Y. Yamamoto, Critical scale invariance in a healthy human heart rate, Phys. Rev. Lett. 93 (2004) 178103. https://doi.org/10.1103/PhysRevLett.93.178103.

[24] K. Kiyono, Z.R. Struzik, N. Aoyagi, Y. Yamamoto, Multiscale probability density function analysis: Non-Gaussian and scale-Invariant fluctuations of healthy human heart rate, IEEE Trans. Biomed. Eng. 53 (2006) 95–102. https://doi.org/10.1109/TBME.2005.859804.

[25] K. Kiyono, J. Hayano, E. Watanabe, Z.R. Struzik, Y. Yamamoto, Non-Gaussian heart rate as an independent predictor of mortality in patients with chronic heart failure, Hear. Rhythm. 5 (2008) 261–268. https://doi.org/10.1016/j.hrthm.2007.10.030.

[26] K. Kiyono, J. Hayano, S. Kwak, E. Watanabe, Y. Yamamoto, Non-gaussianity of low frequency heart rate variability and sympathetic activation: Lack of increases in multiple system atrophy and parkinson disease, Front. Physiol. 3 (2012) 34. https://www.frontiersin.org/article/10.3389/fphys.2012.00034.

[27] J. Hayano, K. Kiyono, Z. Struzik, Y. Yamamoto, E. Watanabe, P. Stein, L. Watkins, J. Blumenthal, R. Carney, Increased non-Gaussianity of heart rate variability predicts cardiac mortality after an acute myocardial infarction, Front. Physiol. 2 (2011) 65. https://doi.org/10.3389/fphys.2011.00065.

[28] L.A. Safonov, Y. Isomura, S. Kang, Z.R. Struzik, T. Fukai, H. Câteau, Near scale-free dynamics in neural population activity of waking/sleeping rats revealed by multiscale analysis, PLoS One. 5 (2010) e12869. https://doi.org/10.1371/journal.pone.0012869.

[29] B.J. West, M. Turalska, Hypothetical control of heart rate variability, Front. Physiol. 10 (2019) 1078. https://doi.org/10.3389/fphys.2019.01078.

[30] D.A. dos Santos, C.A. Fukuchi, R.K. Fukuchi, M. Duarte, A data set with kinematic and ground reaction forces of human balance, PeerJ. 5 (2017) e3626. https://doi.org/10.7717/peerj.3626.

[31] E.A.F. Ihlen, B. Vereijken, Interaction-dominant dynamics in human cognition: Beyond 1/*f* fluctuation, J. Exp. Psychol. Gen. 139 (2010) 436–463. https://doi.org/10.1037/a0019098.

[32] T. Schreiber, A. Schmitz, Improved surrogate data for nonlinearity tests, Phys. Rev. Lett. 77 (1996) 635–638. https://doi.org/10.1103/PhysRevLett.77.635.

[33] J.S. Richman, J.R. Moorman, Physiological time-series analysis using approximate entropy and sample entropy, Am. J. Physiol. Circ. Physiol. 278 (2000) H2039–H2049. https://doi.org/10.1152/ajpheart.2000.278.6.H2039.

[34] J.-H. Ko, K.M. Newell, Aging and the complexity of center of pressure in static and dynamic postural tasks, Neurosci. Lett. 610 (2016) 104–109. https://doi.org/10.1016/j.neulet.2015.10.069.

[35] M. Costa, A.L. Goldberger, C.-K. Peng, Multiscale entropy analysis of complex physiologic time series, Phys. Rev. Lett. 89 (2002) 68102. https://doi.org/10.1103/PhysRevLett.89.068102.

[36] C.-K. Peng, S. V Buldyrev, S. Havlin, M. Simons, H.E. Stanley, A.L. Goldberger, Mosaic organization of DNA nucleotides, Phys. Rev. E. 49 (1994) 1685–1689. https://doi.org/10.1103/PhysRevE.49.1685.

[37] M. Mangalam, R. Chen, T.R. McHugh, T. Singh, D.G. Kelty-Stephen, Bodywide fluctuations support manual exploration: Fractal fluctuations in posture predict perception of heaviness and length via effortful touch by the hand, Hum. Mov. Sci. 69 (2020) 102543. https://doi.org/10.1016/j.humov.2019.102543.

[38] A. Chhabra, R. V Jensen, Direct determination of the *f*(\alpha) singularity spectrum, Phys. Rev. Lett. 62 (1989) 1327–1330. https://doi.org/10.1103/PhysRevLett.62.1327.

[39] M. Mangalam, D.G. Kelty-Stephen, Multiplicative-cascade dynamics supports whole-body coordination for perception via effortful touch, Hum. Mov. Sci. 70 (2020) 102595. https://doi.org/10.1016/j.humov.2020.102595.

[40] K. Kiyono, Z.R. Struzik, Y. Yamamoto, Estimator of a non-Gaussian parameter in multiplicative log-normal models, Phys. Rev. E. 76 (2007) 41113. https://doi.org/10.1103/PhysRevE.76.041113.

[41] D. Bates, M. Mächler, B. Bolker, S. Walker, Fitting linear mixed-effects models using lme4, ArXiv Prepr. ArXiv1406.5823. (2014). https://doi.org/arXiv:1406.5823.

[42] A. Kuznetsova, P.B. Brockhoff, R.H.B. Christensen, lmerTest package: Tests in linear mixed effects models, J. Stat. Softw. 82 (2017) 1548–7660. https://doi.org//10.18637/jss.v082.i13.

[43] W. Lee, K.J. Grimm, Generalized linear mixed-effects modeling programs in R for binary outcomes, Struct. Equ. Model. A Multidiscip. J. 25 (2018) 824–828. https://doi.org/10.1080/10705511.2018.1500141.

[44] I.-C. Lee, M.M. Pacheco, K.M. Newell, Constraints specific influences of vision, touch and surface compliance in postural dynamics, Gait Posture. 59 (2018) 117–121. https://doi.org/10.1016/j.gaitpost.2017.09.014.

[45] K.M. Newell, S.M. Slobounov, E.S. Slobounova, P.C.M. Molenaar, Stochastic processes in postural center-of-pressure profiles, Exp. Brain Res. 113 (1997) 158–164. https://doi.org/10.1007/BF02454152.

[46] M. Duarte, V.M. Zatsiorsky, On the fractal properties of natural human standing, Neurosci. Lett. 283 (2000) 173–176. https://doi.org/10.1016/S0304-3940(00)00960-5.

[47] Y.U. Shimizu, S. Thurner, K. Ehrenberger, Multifractal spectra as a measure of complexity in human posture, Fractals. 10 (2002) 103–116. https://doi.org/10.1142/S0218348X02001130.

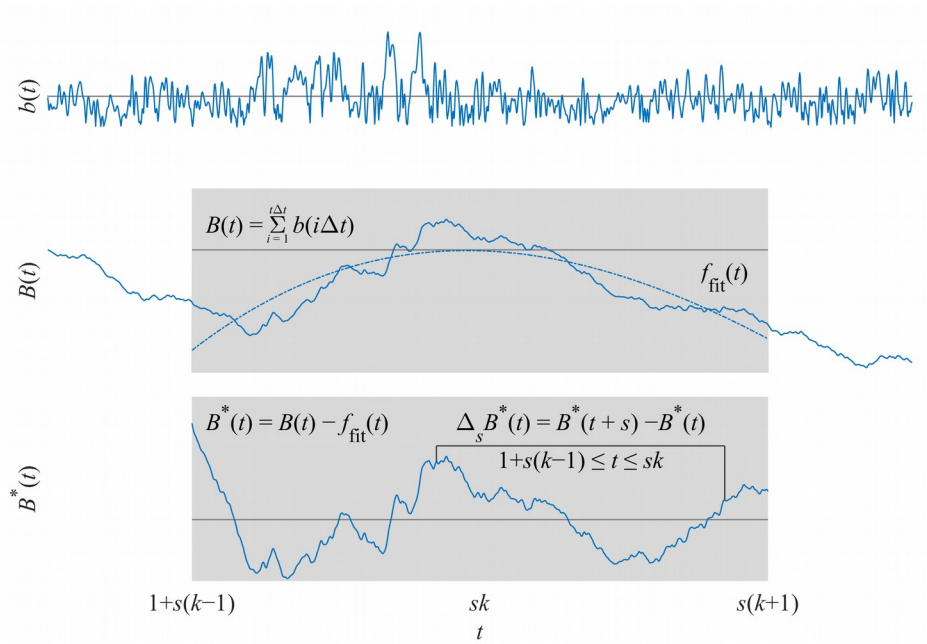

Fig. 1. Schematic illustration of multiscale probability density function (PDF) analysis. Top: The first step is to generate { $B(t)$ } by integrating { $b(t)$ } after centering by the mean b_{ave} : $B(t)=\sum_{i=1}^{t/\Delta t} b(i\Delta t)-b_{ave}$. Middle: A a 3rd order polynomial detrends { $B(t)$ } within k overlapping windows of length $2s$, s being the timescale. Bottom: Intermittent deviation $\Delta_s B(t)$ in k^{th} window from $1+s(k-1)$ to sk in the detrended time series { $B^d(t)=B(t)-f_{fit}(t)$ } is computed as $\Delta_s B^d(t)=B^d(t+s)-B^d(t)$, where $1+s(k-1)\le t\le sk$ and $f_{fit}(t)$ is the polynomial representing the local trend of { $B(t)$ }, of which the elimination assures the zero-mean probability density function in the next step.

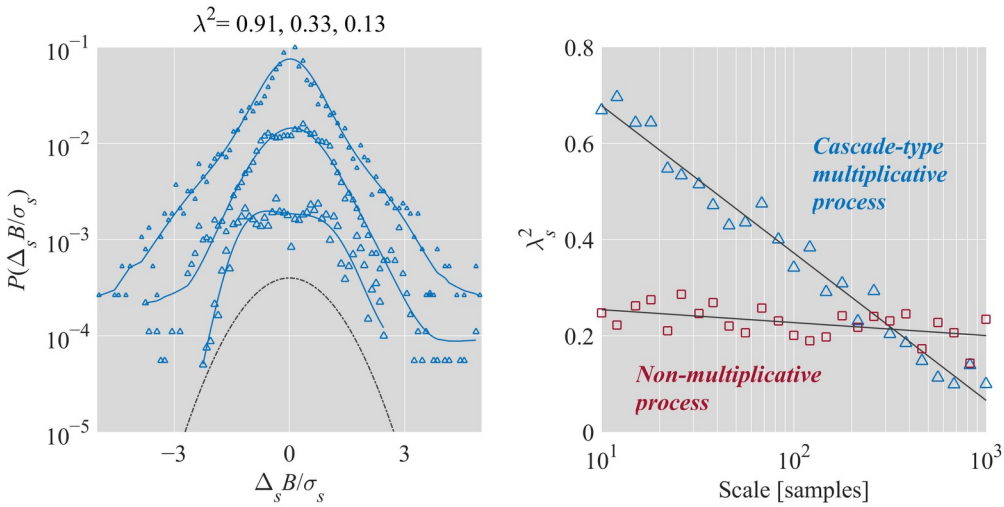

Fig. 2. Schematic illustration of non-Gaussianity index λ_s . Left: The relationship between λ_s^2 and shapes of PDF plotted in linear-log coordinates for λ_s^2 = 0.9, 0.33, and 0.13 (from top to bottom). For clarity, the PDFs have been shifted vertically. As λ_s^2 increases, the PDF becomes increasingly peaked and fat-tailed. As λ_s decreases, the PDF increasingly resembles the Gaussian (dashed line), assuming a perfect Gaussian as λ_s^2 approaches 0. Right: In a cascade-type multiplicative process yield the inverse relationship $\lambda_s^2 \sim -\ln s$.

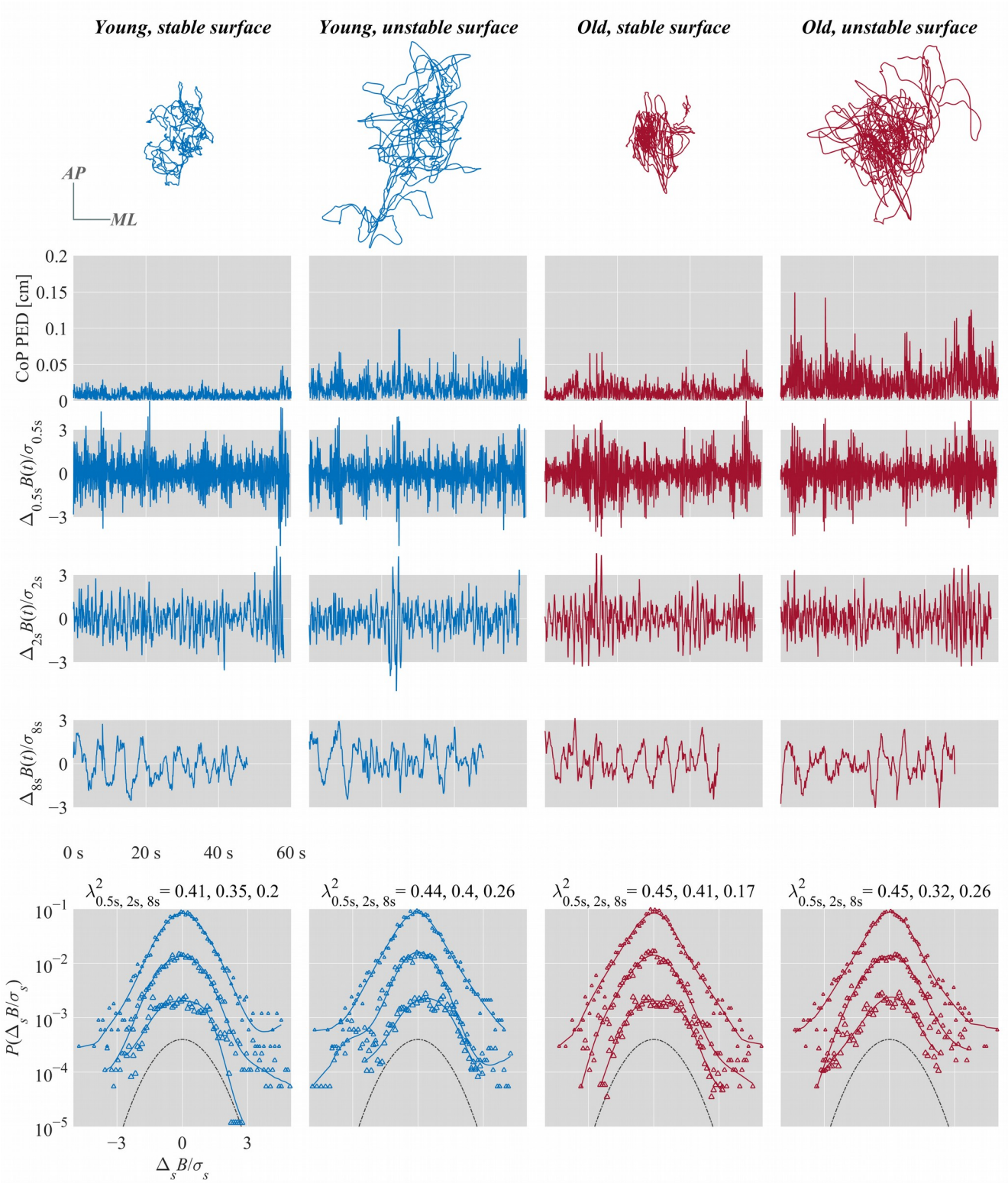

Fig. 3. Multiscale PDF characterization of postural sway in representative young and old participants standing quietly for 60 s on stable and unstable surfaces with their eyes open. From top to bottom: CoP trajectories along the anterior-posterior (*AP*) and medial-lateral (*ML*) axes. CoP PED series. { $\Delta_s B(i)$ } for s = 0.5, 2, and 8 s. Standardized PDFs (in logarithmic scale) of { $\Delta_s B(i)$ } for s = 1, 2, and 4 s (from top to bottom), where σ_s denotes the *SD* of { $\Delta_s B(i)$ }.

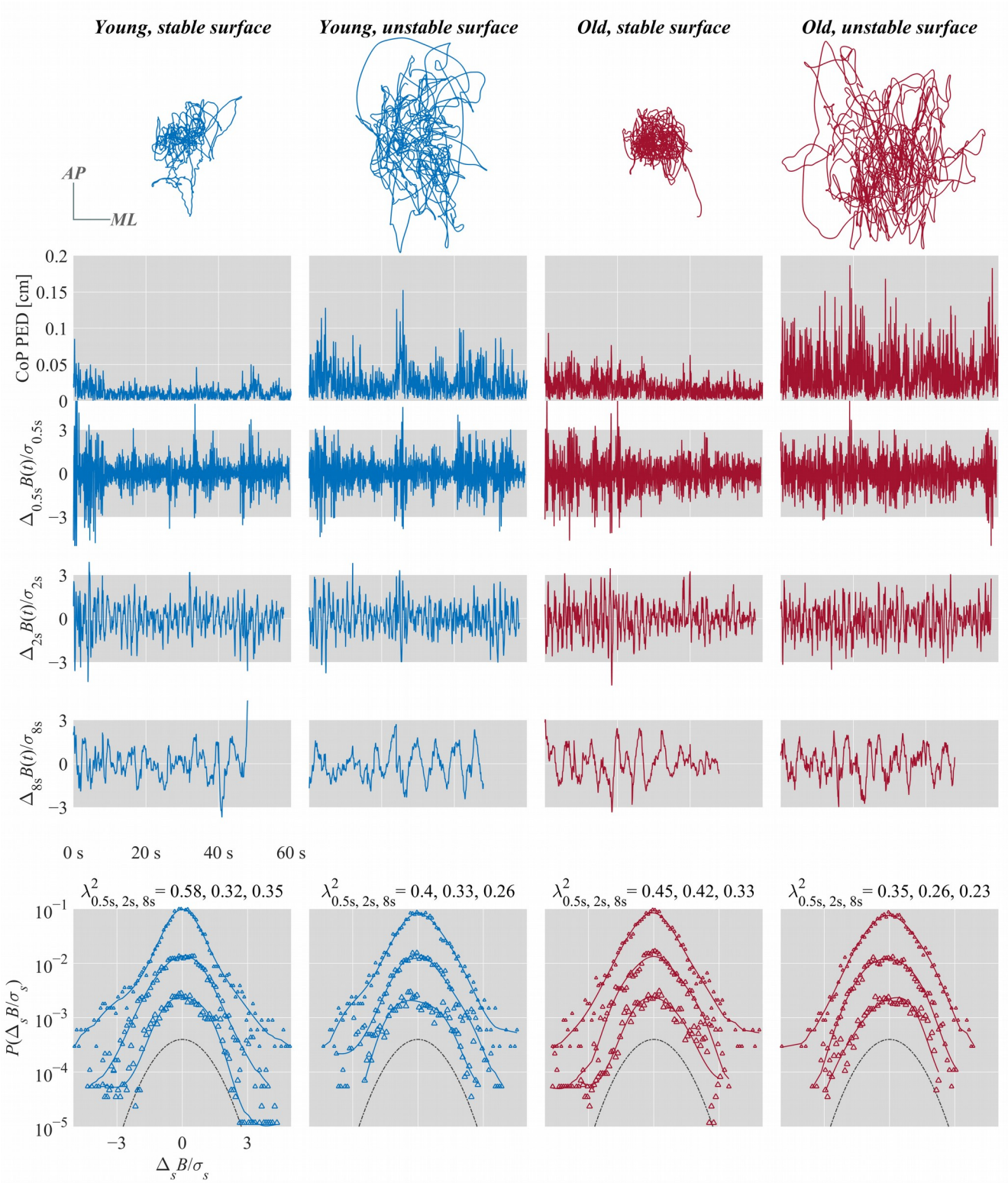

Fig. 4. Multiscale PDF characterization of postural sway in representative young and old participants standing quietly for 60 s on stable and unstable surfaces with their eyes closed. From top to bottom: CoP trajectories along the anterior-posterior (*AP*) and medial-lateral (*ML*) axes. CoP PED series. { $\Delta_s B(i)$ } for s = 0.5, 2, and 8 s. Standardized PDFs (in logarithmic scale) of { $\Delta_s B(i)$ } for s = 1, 2, and 4 s (from top to bottom), where σ_s denotes the *SD* of { $\Delta_s B(i)$ }.

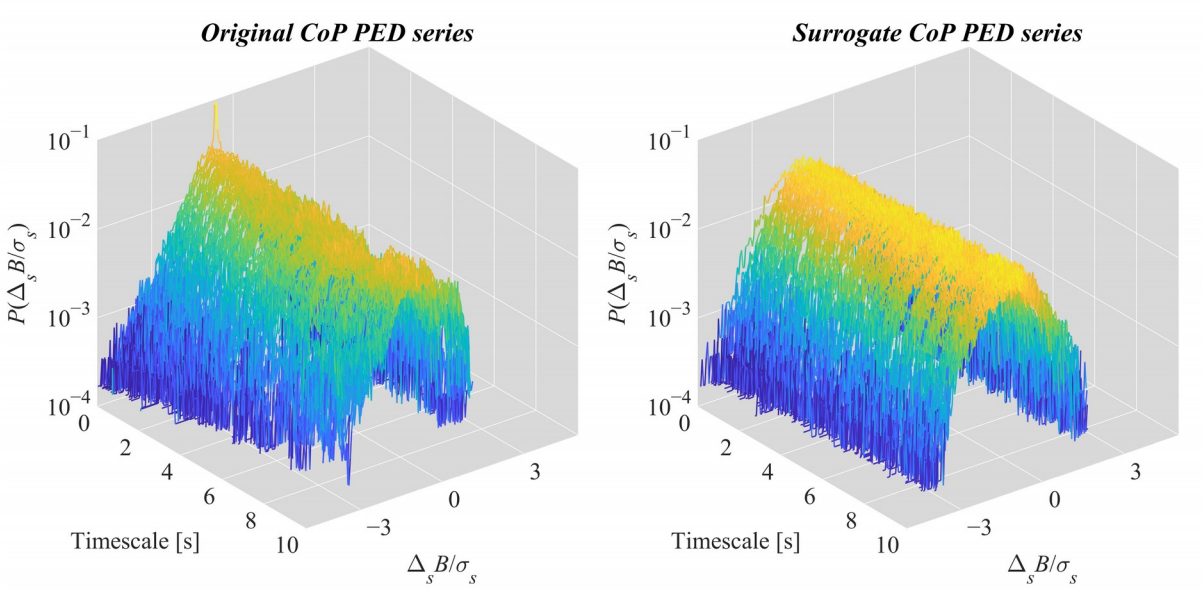

Fig. 5. PDFs at timescales ranging from 50 ms to 10 s, obtained from multiscale PDF analysis for a representative original CoP PED series and its IAAFT surrogate.

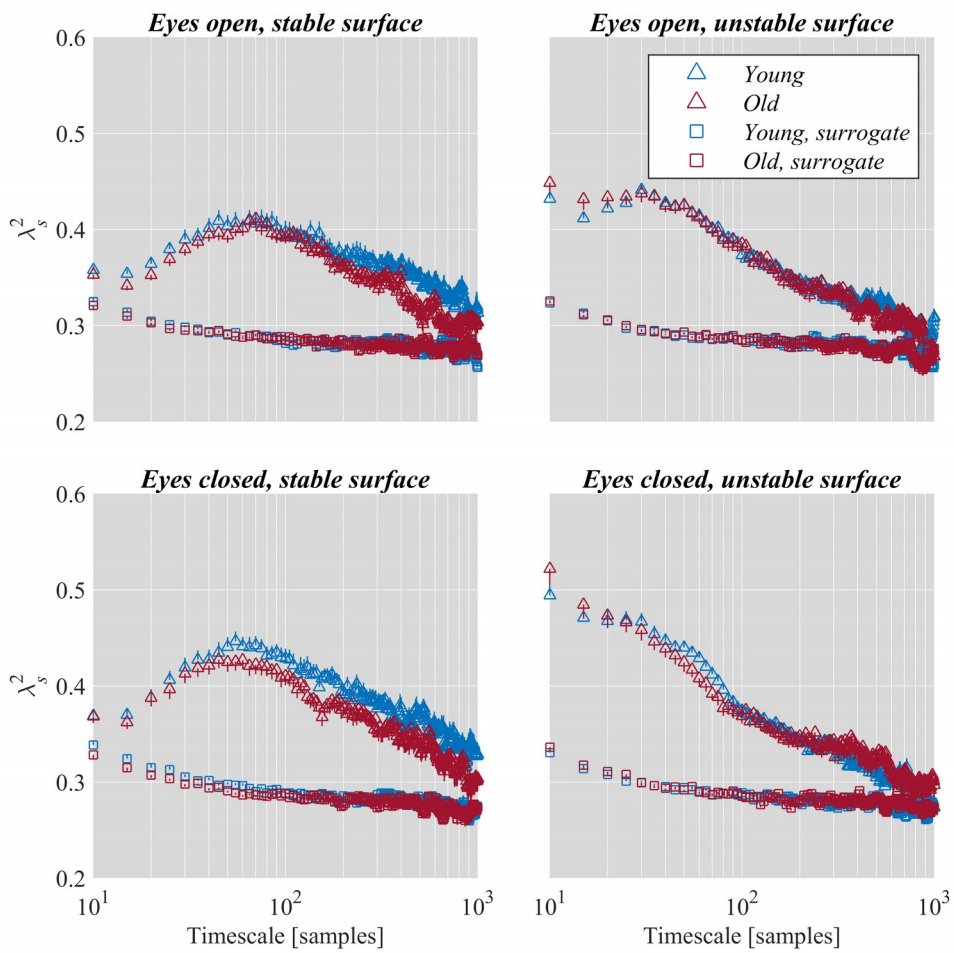

Fig. 6. Timescale dependence of the non-Gaussianity index λ_s^2. Mean values of λ_s^2 for the young and old participants maintaining upright balance for 60 s on stable and unstable surfaces with their eyes open and eyes closed. Vertical bars indicate ±1*SEM* of the group averages (Young, *N* = 27; Old, *N* = 22).

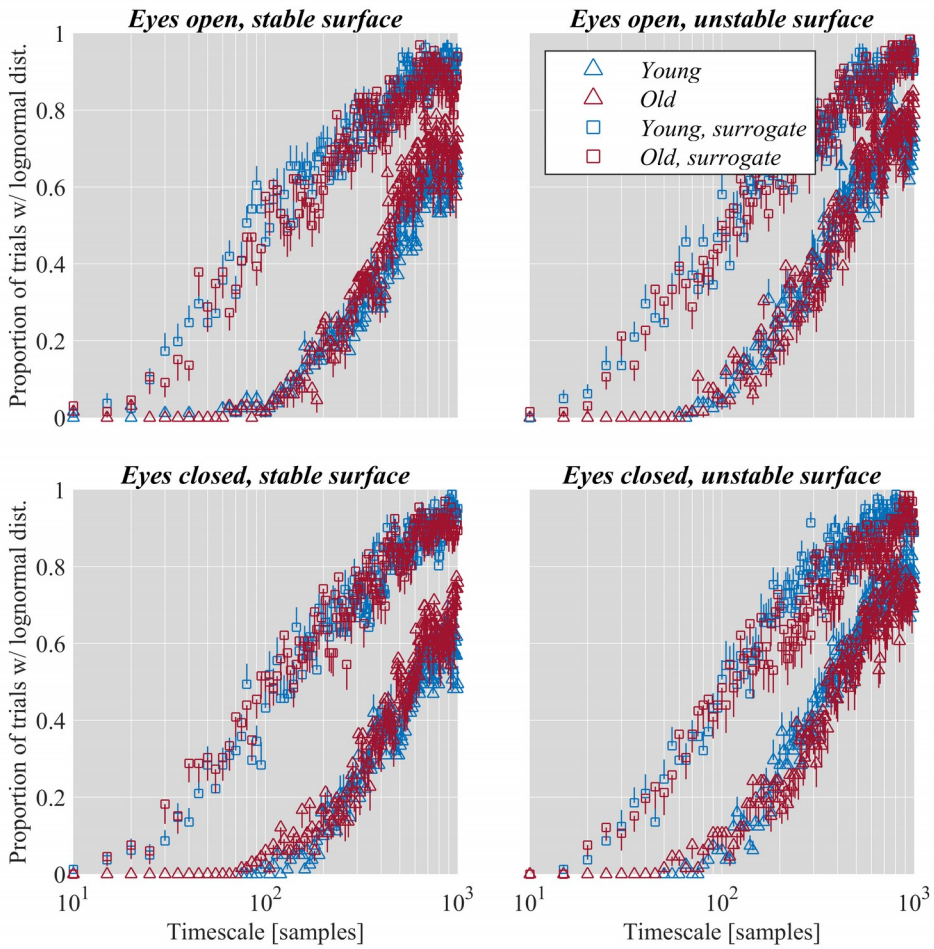

Fig. 7. Timescale dependence of the mean proportion of trials with a lognormal distribution for the young and old participants maintaining upright balance for 60 s on stable and unstable surfaces with their eyes open and eyes closed. Vertical bars indicate ±1*SEM* of the group averages (Young, N = 27; Old, N = 22).